Influence of Ti-Mo addition on the hydrogen embrittlement resistance of Fe-5.6Mn-0.16C-1Al steel

Jianglong Pan, Shuyi Wang, Rui Liu and Minghui Cai†

School of Materials Science and Engineering, Northeastern University, Shenyang 110819, China

†E-mail: caimh@smm.neu.edu.cn

www.neu.edu

Due to the introduction of hydrogen, there is a serious hydrogen embrittlement problem, which will make the material embrittlement and affect the service life and safety of steel. Therefore, the effect of adding Ti-Mo on the hydrogen embrittlement susceptibility of medium Mn steel was studied in this paper to improve the hydrogen embrittlement resistance. The hydrogen embrittlement susceptibility of 5.6Mn/5.6MnTiMo steel was studied after heat treatment at 670 ℃ for 30 min. The results show that the addition of Ti-Mo can form (Ti, Mo) C carbide to increase the stability of austenite, and the TRIP effect slows down during deformation, so that 5.6MnTiMo steel exhibits higher hydrogen embrittlement resistance. SEM analysis shows that the fracture morphology of the H-uncharged samples is ductile fracture, showing a small hollow dimple. The H-charged samples is "hydrogen-induced" brittle fracture, showed a mixture of solid dimple and intergranular fracture.

Keywords: Warm-rolled medium Mn steel; Ti-Mo microalloying; Critical heat treatment; Hydrogen embrittlement; Austenite stability.

1. Introduction

The research and development idea of the third generation of advanced high-strength steel for automobiles - medium Mn steel is to generate a ferrite matrix with sufficient strength and a sufficient and stable residual austenite (>30 %), which can produce TRIP effect during the strain process and obtain excellent mechanical properties[1]. In recent years, with the increasing strength level of materials, the hydrogen embrittlement problem of Mn steel has become increasingly prominent[2-5]. In addition, the plastic deformation of medium Mn steel will occur during the process of manufacturing and service, and a large amount of austenite will be transformed into high carbon martensite, which may lead to a more serious hydrogen embrittlement problem. Han[2] et al. compared the hydrogen embrittlement resistance of hot-rolled and cold-rolled manganese steel, and found that the plastic loss of the two was as high as 89 % and 74 %, respectively, the fracture showed intergranular fracture. Ryu and Han[2, 6] et al. found that the austenitic stability of medium Mn steel is proportional to the hydrogen embrittlement resistance.

† The authors gratefully acknowledge the financial support of the Natural Science Foundation of China (Nos. 51975111/52274379), Key R&D and Promotion Special Project of Henan Province (No. 212102210444) and the Fundamental Research Funding of the Central Universities (2023GFZD14). Special thanks are due to the instrumental/data analysis from Analytical and Testing Center, Northeastern University.

Y. Zhang and M. Ma (eds.), *Proceedings of the 7th International Conference on Advanced High Strength Steel and Press Hardening (ICHSU 2024)*, Atlantis Highlights in Materials Science and Technology 3,
https://doi.org/10.2991/978-94-6463-581-2_34

Therefore, in order to improve the hydrogen embrittlement resistance of medium Mn steel, this study added Ti-Mo microalloying element on the basis of Fe-5.6Mn-0.16C-1Al(wt.%) steel, systematically compared the hydrogen embrittlement resistance and microstructure evolution of the two experimental steels.

2. Experimental procedures

2.1. *Experimental material*

The two experimental steels were Fe-5.6Mn-0.2C-1Al steel and Fe-5.6Mn-0.2C-1Al-0.08Ti-0.22Mo steel. The ingot was solubilised at 1200 ℃ for 2 h, then hot rolled into a 5mm thick sheet in the temperature range of 1100 ℃~900 ℃, and air-cooled to room temperature. The sheet is kept warm at 630 ℃ for 10 min, then rolled into 1.5mm thick sheet after 5 passes. Finally, the warm rolled plates were critically heat treated at 670℃ for 30min, air cooled to room temperature.

2.2. *Materials characterization*

In order to evaluate the hydrogen embrittlement susceptibility of the experimental steel, the slow tensile rate was set to $5*10^{-5}$ s^{-1}, the H-charged current density is 0.2 mA/cm^2 and the time is 1h. Microstructure was characterized by X-ray Diffraction (XRD;RIGAKU,D/MAX-2000), field emission scanning electron microscopy (FE-SEM, JEOL, JSM-7000F) and Electron Backscattered Diffraction (EBSD; Oxford, NordlysNano).The susceptibility of hydrogen embrittlement can be assessed by strength loss (I_δ) and plasticity loss (I_σ):

$$I_\delta = \frac{\delta_{Air}\text{-}\delta_H}{\delta_{Air}} \times 100\% \quad (1)$$

$$I_\sigma = \frac{\sigma_{Air}\text{-}\sigma_H}{\sigma_{Air}} \times 100\% \quad (2)$$

where δ_{Air}, σ_{Air} and δ_H, σ_H are the total elongation (TEL) and ultimate tensile strength (UTS) of the H-uncharged and H-charged specimens.

3. Results

3.1. *Mechanical properties*

As shown in Fig.1, the addition of Ti-Mo microalloying elements not only improves the strength of the experimental steel, but also enhances the hydrogen embrittlement resistance of the experimental steel. Compared with 5.6Mn steel, the yield strength of 5.6MnTiMo steel increases by about 236 MPa due to the addition of Ti-Mo. In addition, when the H-charged current density is 0.2 mA/cm^2, the I_δ and I_σ of 5.6Mn steel are 23 % and 15 %, the I_δ and I_σ of 5.6MnTiMo steel are only 2 % and 6 %.

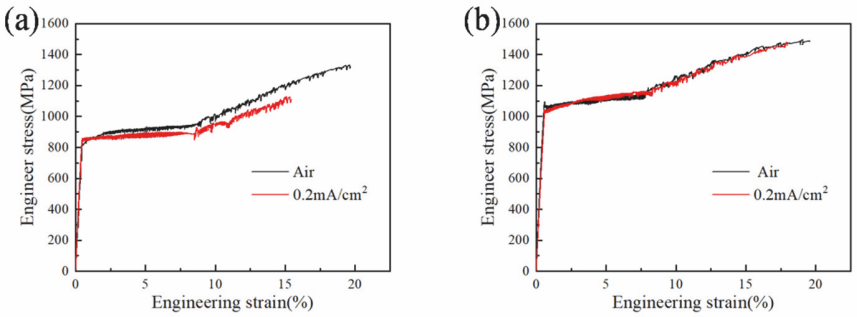

Fig. 1. The engineering stress-strain curves of H-uncharged and H-charged (a) 5.6Mn steel and (b) 5.6MnTiMo steel.

3.2. *Microstructures Characterization*

Fig.2 shows the EBSD diagram of 5.6Mn steel and 5.6MnTiMo steel after annealing at 670 ℃ for 30 min respectively. On the image quality (IQ)-phase maps, the red and blue phases correspond to α and γ_R; while the white and black lines represent low angle grain boundaries (2 °-15 °) and high angle grain boundaries (>15 °), respectively. After critical heat treatment, all the samples showed α and γ_R ultrafine crystalline microstructure. the addition of Ti-Mo microalloying elements, on the one hand, can increase the proportion of low angle grain boundaries in the experimental steel. on the other hand, reduce the average grain size of the experimental steel, especially the average grain size of the α phase. For example, the average grain size of α phase in 5.6Mn steel is 1.16 μm, but the average grain size of α phase in 5.6MnTiMo steel is reduced to 0.98 μm. The average grain size calculated by AZtecCrystal is shown in Table 1.

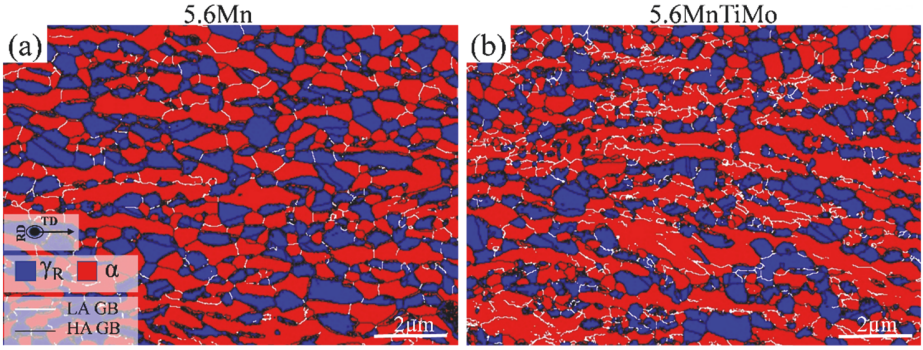

Fig. 2. EBSD IQ-phase map of 5.6Mn steel and 5.6MnTiMo steel after critical heat treatment for 30min.

Table 1 Grain size of 5.6Mn steel and 5.6MnTiMo steel.

Steels	Grain size(μm)	670 ℃
5.6Mn	α	1.16
	γ_R	0.78
5.6MnTiMo	α	0.98
	γ_R	0.71

4. Discussion

4.1. *Characteristic of fracture*

In order to clarify the cause of premature fracture of H-charged samples, SEM fracture images of 5.6Mn steel/5.6MnTiMo steel H-uncharged and H-charged samples were observed respectively. As shown in Fig.3, the fractures of all samples H-uncharged showed obvious delamination phenomenon and necking shrinkage, and showed small hollow dimples and typical ductile fractures at high magnification.

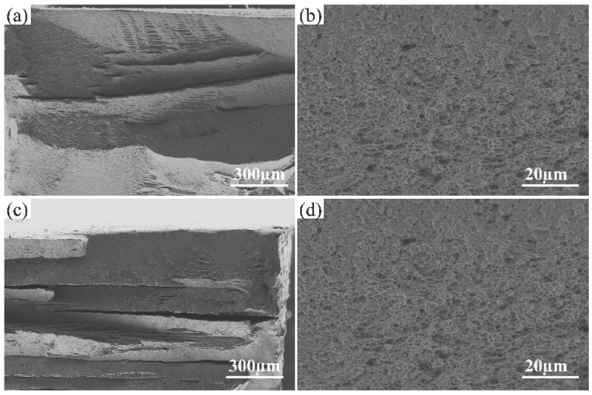

Fig. 3. SEM fractography of H-uncharged (a,b) 5.6Mn steel and (c,d) 5.6MnTiMo steel.

SEM fracture images of H-charged samples were taken near the center of the fracture surface, as shown in Fig.4, fractures of all H-charged samples are typical "hydrogen-induced" brittle fractures, and the surface seems to be covered with small pits. Under high magnification, the fracture surface showed a mixture of solid dimple and intergranular fracture.

Based on the fact that H-uncharged samples only show ductile fracture, it is believed that hydrogen brittle fracture leads to premature fracture of H-charged samples.

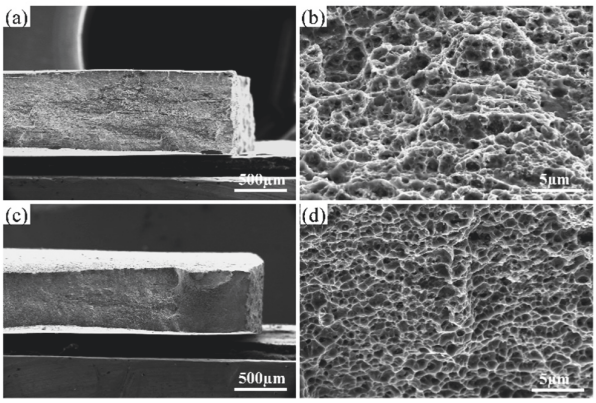

Fig. 4. SEM fractographs of H-charged (a,b) 5.6Mn steel and (c,d) 5.6MnTiMo steel.

4.2. *Effect of Ti-Mo addition on hydrogen embrittlement susceptibility*

Zhang[7] et al and Shao[8] et al found that the hydrogen embrittlement susceptibility of medium Mn steel decreases with the increase of austenite stability. As shown in Fig.5, the two points respectively represent the austenite volume fraction of the undeformed samples and the H-uncharged tensile fracture samples. The stability of austenite can be evaluated by k, and the value of k is inversely proportional to the stability of austenite. k can be calculated by formula **(3)**[9] :

$$k = -\frac{ln\left(\frac{V_{RA}}{V_{RA0}}\right)}{\varepsilon} \tag{3}$$

Where V_{RA0} is the γ_R volume fraction before the strain, V_{RA} is the γ_R volume fraction when the strain is ε, k is the mechanical stability of γ_R. The of 5.6Mn steel and 5.6MnTiMo steel is 18.8 and 12.6, respectively, which indicates that the austenite of 5.6Mn steel is more stable than that of 5.6Mn steel.

In this study, with the addition of Ti-Mo microalloying elements, austenite stability is enhanced, TRIP effect is slowed down during tensile process, and hydrogen-assisted cracking is delayed. Thus, 5.6MnTiMo steel exhibits higher resistance to hydrogen embrittlement.

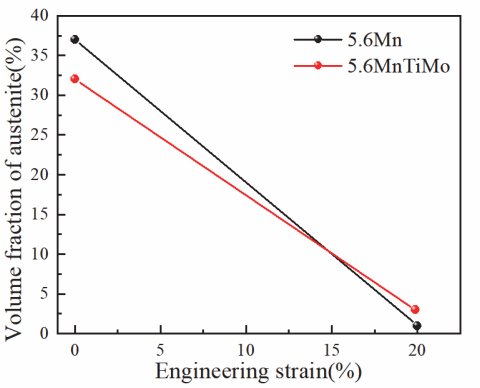

Fig. 5. 5.6Mn Steels and 5.6MnTiMo steels austenite volume fraction along with the change of engineering strain.

5. Conclusions

Due to the addition of Ti-Mo, the 5.6MnTiMo steel has a more stable γ_R, and the TRIP effect will be slowed down during the deformation process of the experimental steel, that is, the transformation from austenite to martensite will be weakened, so that the addition of Ti-Mo microalloy element can improve the hydrogen embrittlement resistance on the premise of greatly improving the strength of the experimental steel.

References

1. Y.-b. Xu, Z.-p. Hu, Y. Zou, X.-d. Tan, D.-t. Han, S.-q. Chen, D.-g. Ma, R.D.K. Misra, Effect of two-step intercritical annealing on microstructure and mechanical properties of hot-rolled medium manganese TRIP steel containing δ-ferrite, Materials Science and Engineering: A 688 (2017) 40-55.
2. J. Han, J.-H. Nam, Y.-K. Lee, The mechanism of hydrogen embrittlement in intercritically annealed medium Mn TRIP steel, Acta Materialia 113 (2016) 1-10.
3. J.H. Ryu, Y.S. Chun, C.S. Lee, H.K.D.H. Bhadeshia, D.W. Suh, Effect of deformation on hydrogen trapping and effusion in TRIP-assisted steel, Acta Materialia 60(10) (2012) 4085-4092.
4. X. Zhu, W. Li, T.Y. Hsu, S. Zhou, L. Wang, X. Jin, Improved resistance to hydrogen embrittlement in a high-strength steel by quenching–partitioning–tempering treatment, Scripta Materialia 97 (2015) 21-24.
5. H.K.D.H. Bhadeshia, Prevention of Hydrogen Embrittlement in Steels, ISIJ International 56(1) (2016) 24-36.
6. J.H. Ryu, Y.S. Chun, C.S. Lee, H. Bhadeshia, D.W. Suh, Effect of deformation on hydrogen trapping and effusion in TRIP-assisted steel, Acta Materialia 60(10) (2012) 4085-4092.
7. Y. Zhang, W. Hui, X. Zhao, C. Wang, W. Cao, H. Dong, Effect of reverted austenite fraction on hydrogen embrittlement of TRIP-aided medium Mn steel (0.1C-5Mn), Engineering Failure Analysis 97 (2019) 605-616.
8. C. Shao, W. Hui, Y. Zhang, X. Zhao, Y. Weng, Effect of intercritical annealing time on hydrogen embrittlement of warm-rolled medium Mn steel, Materials Science and Engineering: A 726 (2018) 320-331.
9. Z.H. Cai, H. Ding, R.D.K. Misra, Z.Y. Ying, Austenite stability and deformation behavior in a cold-rolled transformation-induced plasticity steel with medium manganese content, Acta Materialia 84 (2015) 229-236.